**Pd/C-CeO$_2$ anode catalyst for high performance platinum free anion exchange membrane fuel cells†**

Hamish A. Miller,*[a] Alessandro Lavacchi,[a] Francesco Vizza, *[a] Marcello Marelli , [c] Francesco Dei Benedetto,[f] Francesco D'Acapito,[g] Yair Paska,[b] Miles Page,[b] and Dario R. Dekel*[d,e]

[a] Istituto di Chimica dei Composti Organometallici (CNR-ICCOM), via Madonna del Piano 10, 50019 Sesto Fiorentino, Firenze, Italy.
[b] CellEra, Caesarea Business and Industrial Park, Caesarea, 30889, Israel.
[c] Istituto di Scienze e Tecnologie Molecolari (ISTM-CNR) via Camillo Golgi 19, 20133 Milano.
[d] The Wolfson Department of Chemical Engineering, Technion – Israel Institute of Technology, Haifa, 3200003, Israel.
[e] The Nancy & Stephan Grand Technion Energy Program (GTEP), Technion – Israel Institute of Technology, Haifa 3200003 Israel.
[f] Department of Earth Sciences, Università di Firenze, Via G. La Pira, 4, 50100 Firenze, Italy.
[g] CNR-IOM-OGG c/o ESRF, 71, Avenue des Martyrs, CS, 40220 Grenoble, Cédex 9, France.

**Abstract:**

Removal of platinum from polymer electrolyte membrane fuel cells is one of the most commonly cited objectives for researchers in this field. Here we describe a platinum free anion exchange membrane fuel cell (AEM-FC) that employs nanostructured Pd anode and Ag cathode electrocatalysts. AEM-FC tests run on dry hydrogen and pure air show peak power densities of more than 500 mW cm$^{-2}$. Such high power output is shown to be due to a nanoparticle Pd anode catalyst with a composite Vulcan XC-72 carbon-CeO$_2$ support that exhibits enhanced kinetics for hydrogen oxidation in alkaline media.

The fuel cell is considered the best device for converting the chemical energy of hydrogen cleanly into electricity on demand with the only byproducts water and heat. State of the art low temperature proton exchange membrane fuel cells (PEM-FCs) are compact systems with high power densities, which make them ideal for automotive applications. Recent analyses have shown that among PEM-FC components around 56% of the cost comes from the platinum electrocatalyst.[1, 2] Therefore, a complete removal of platinum in fuel cell stacks and replacement with metals that are less expensive and more abundant in nature is crucial to make this technology an affordable solution for automotive as well as other large scale applications.

As an alternative to PEM-FCs that work under highly corrosive acidic conditions and require high loadings of Pt catalysts, the alkaline anion exchange membrane fuel cell (AEM-FC) has long been proposed as a solution to reduce costs by avoiding the use of platinum.[3-10] Fig. 1 shows a schematic representation of the AEM-FC presented in this work.
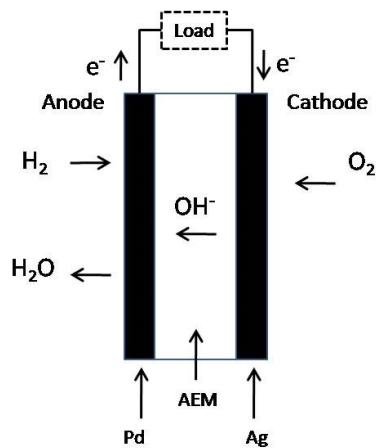


Fig. 1. Schematic representation of the Pt-free AEM-FC.

Regarding the cathode catalyst, platinum can be readily replaced by palladium[11, 12] and (?) non-noble metals.[8, 13-24] The range of materials used include transition metal phthalocyanines,[25, 26] heat treated (600-1000 °C) carbon supported metal phthalocyanines,[25-30] materials derived from carbon supported metal and nitrogen precursors heat treated under inert atmosphere (600-1000 °C)[31, 32] and nitrogen doped carbon materials that may or may not contain transition metals.[33-35] Widely used in liquid electrolyte Alkaline Fuel Cells (AFCs), nanostructured Ag catalysts have also been

extensively investigated.[36-38, 39-41] The range of available AEMs and ionomers that have been investigated for electrochemical systems including AEM-FCs has been recently comprehensively reviewed by Varcoe *et al.*[10] Relatively less attention has been paid to the anode catalyst where the hydrogen oxidation reaction (HOR) occurs.[3, 9, 42-45] In stark contrast to PEM-FCs, the kinetics of the HOR reaction is quite slow under alkaline conditions even when Pt is used. Indeed, the HOR activity on carbon supported noble metals (Pt, Pd and Ir) decreases by circa 100x when switching from low to high pH.[46] This factor has been the main stumbling block preventing the realization of a Pt free AEM-FC with useful power output. Since Lu and co-workers first presented a noble metal free AEM-FC in 2008 ($H_2/O_2$, $T_{cell}$ 60 °C, maximum power density 50 mW $cm^{-2}$),[3, 24] little progress has been made primarily due to the challenge of overcoming poor HOR kinetics in alkaline AEM-FCs.

In this work we present a nanoparticle Pd anode catalyst with a composite Vulcan XC-72 carbon-$CeO_2$ support which exhibits enhanced kinetics for the HOR in alkaline conditions. The mixed $CeO_2$/carbon support was prepared by depositing 50 wt% $CeO_2$ onto Vulcan XC-72 carbon.[47] The desired amount of Pd (10 wt%) was deposited by the addition of a Pd(II) precursor to a suspension of this support under aqueous alkaline conditions followed by reduction with ethanol at 80 °C (see the SI for complete synthetic details and XRPD characterization).

The Pd/C-$CeO_2$ anode catalyst and a reference homemade Pd/C were incorporated into anode catalyst layers (0.30 $mg_{Pd}$ $cm^{-2}$), and together with a Ag cathode catalyst (3.0 $mg_{Ag}$ $cm^{-2}$), anion exchange membrane and ionomer, membrane electrode assemblies (MEAs)[48] were prepared for testing in AEM-FC single cells (see SI for complete description).[18-22] Fig. 2 shows the cell performance at 73 °C with dry $H_2$ at the anode and humidified filtered air (<10 ppm $CO_2$) at the cathode.
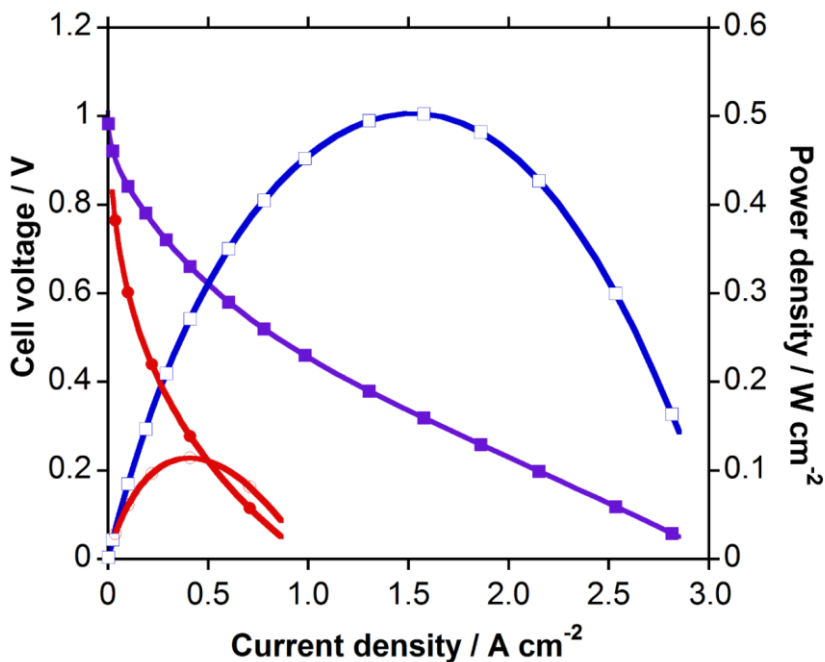
Fig. 2: Typical voltage and power density (*vs*. current density) curves of MEAs with Pd/C (red curves) and Pd/C-CeO$_2$ (blue curves) anodes (0.30 mg$_{Pd}$ cm$^{-2}$). T$_{cell}$ = 73 °C. The cathode in all tests is a Ag catalyst (cathode loading 3 mg$_{Ag}$ cm$^{-2}$). Cathode feed air 1 slm (<10ppm CO$_2$);  Anode fuel dry H$_2$ (0.2 slm).

      The AEM-FC containing the  Pd/C anode catalyst performed modestly in cell tests reaching a maximum power density of slightly above 0.1 W cm$^{-2}$ and maximum current density of ~ 1 A cm$^{-2}$. With the same electrode Pd loading (0.3 mg$_{Pd}$ cm$^{-2}$) as the carbon supported catalyst, the C-CeO$_2$ supported catalyst reaches a peak power density of 0.5 W cm$^{-2}$ at a current density of about 1.5 A cm$^{-2}$ and a maximum current density of ca. 3 A cm$^{-2}$. A clear significantly higher fuel cell performance is obtained switching the carbon support for the C-CeO$_2$ support. In order to gain a clear understanding of the origin of the ameliorative effect of CeO$_2$ on the HOR activity of Pd, we have investigated the electrochemical activity in half cell tests. Cyclic voltammetry (CV) curves obtained in static N$_2$ saturated 0.1 M KOH for Pd/C and Pd/C-CeO$_2$ are shown in Fig. 3a. The peaks for hydrogen adsorption and desorption (UPD) processes can be readily assigned by comparison with literature data.[47] A cathodic shift in the H$_{UPD}$ oxidation peak (circa 90 mV) can be seen for the C-CeO$_2$ supported catalyst with respect to the carbon supported catalyst (evidenced in Figure 3a). This implies that H is bound less strongly on the C-CeO$_2$

supported Pd surface. A weakening of the metal-hydrogen (M-H) binding energy is known to lead to enhancements in HOR kinetics under alkaline conditions.[49-51] In fact, the rate determining step of the HOR in alkaline conditions is considered to be the oxidative desorption of H.[50] Indeed, we observe an increase in the HOR activity of Pd/C-CeO₂ with respect to Pd/C (evaluated with a rotating disk electrode in $H_2$ saturated 0.1 M aqueous KOH in Figure 3b). The Pd/C catalyst exhibits typically sluggish HOR kinetics not reaching the diffusion limited current plateau below 0.5 V (RHE).[50, 52] By contrast the Pd/C-CeO₂ catalyst shows enhanced HOR activity reaching the diffusion limited current plateau at circa 0.25 V.
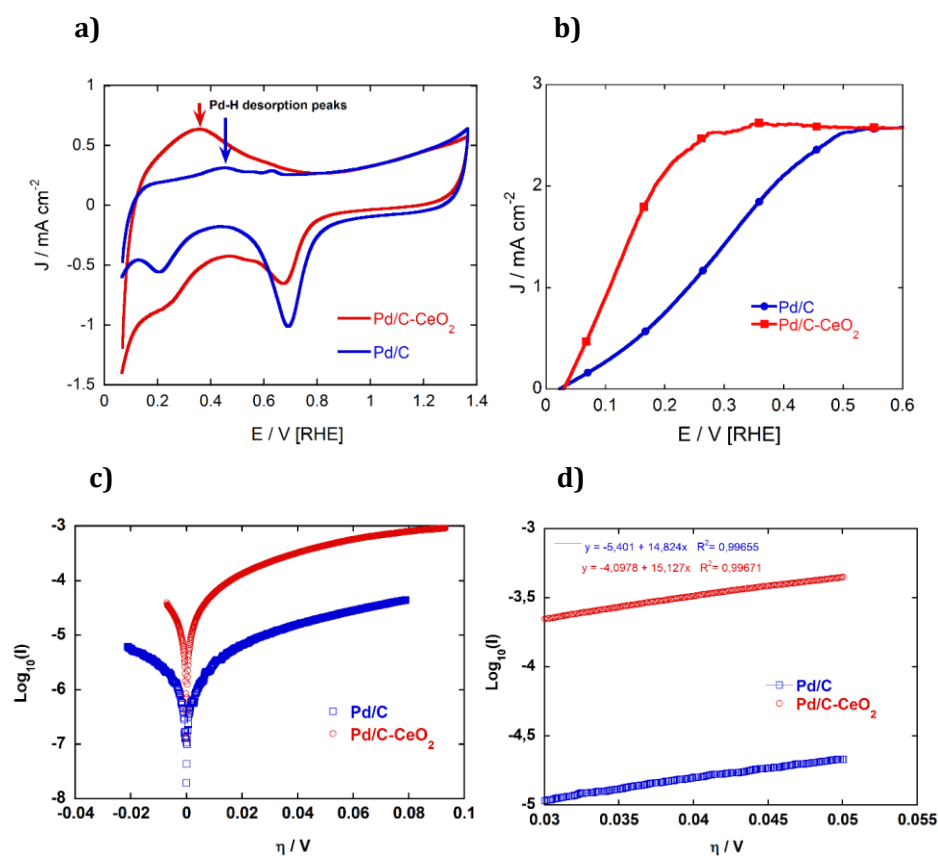


Fig. 3: (a) Cyclic voltammetry of Pd/C and Pd/C-CeO₂ in static $N_2$ saturated 0.1 M KOH solution, (b) Steady state polarization curves of HOR in $H_2$ sat 0.1 M KOH (1600 RPM), (c) Tafel slope analysis for in $H_2$-saturated, 0.1 M KOH obtained at 10 mV s$^{-1}$ and 2500 rpm and (d) linear fits of the kinetic current at high current density.

Tafel analysis was used to study the HOR reaction on each of the catalyst surfaces (Fig. 3c). Tafel plots were obtained by correcting the HOR branch of the data by subtracting the diffusion overpotential and determining the kinetically limited HOR currents.[53] Electrochemical data are also shown in Table 1, including the electrochemically active surface areas (EASA), exchange current densities and the mass activity per gram of Pd. The Tafel slopes were determined from linear fits of the kinetic currents at high current density (Fig. 3d). The exchange current density for the HOR increases more than 20 fold for Pd/C-CeO$_2$ catalyst with respect to Pd/C. Both catalysts have a similar EASA and Pd particle size distribution (see SI for representative TEM micrographs of Pd/C), so such an increase in activity must be due to electronic effects due to the Pd-CeO$_2$ interaction. Tafel slopes are also similar for both catalysts suggesting the same HOR mechanism on both surfaces (66-68 mV dec$^{-1}$).

**Table 1** Electrochemical data.

| | $i_{0, m}$ (A g$_{Pd}^{-2}$) | $i_0$ (mA. cm$_{Pd}^{-2}$) | EASA m$^2$ g$^{-1}_{Pd}$ | Tafel slope mV dec$^{-1}$ |
|---|---|---|---|---|
| Pd/C | 1.1 | 2.7 | 45 | 68 |
| Pd/C-CeO$_2$ | 24 | 54.5 | 43 | 66 |

The promotional effect of the Pd-CeO$_2$ combination on the HOR is also due to an oxophilic effect. Ceria (CeO$_2$) is one of the most recognized oxygen deficient compounds.[54] Ceria has been widely employed as oxide promoter on both the anode side of fuel cells through enhancement of the CO tolerance of Pt and for the enhancement of the ORR on Pt in fuel cell cathodes.[55-57] We have found in previous studies that a mixed ceria-carbon support enhances the activity of Pd anodes in Direct Ethanol Fuel Cells (DEFCs) by promoting the formation at low potentials of the Pd$^I$OH$_{ads}$ species that are responsible for ethanol electrooxidation.[47] To the best of our knowledge the application of CeO$_2$ in promoting the HOR has not been yet reported. Saturation of the CeO$_2$ surface with OH$^-$ ions is very rapid in alkaline media and likewise the spillover of OH$^-$ to the Pd nanoparticles in close proximity.[58] In a recent paper Markovic and co-workers demonstrated that the HOR rate can be improved dramatically by optimizing the balance between the active sites required for the adsorption and dissociation of H$_2$ (noble metal e.g. Pt or Pd) and the adsorption of hydroxyl species (OH$_{ad}$) in this example on RuO$_2$.[59] Such spillover phenomena and consequent enhancement of the HOR will naturally be magnified by an intimate contact between the three components of the catalyst; ceria, Pd and carbon. This effect has to be justified by an intimate contact of the palladium nanoparticles with CeO$_2$.

We have used high angle annular dark field (HAADF) scanning transmission electron microscopy (STEM) and high resolution transmission electron microscopy (HRTEM) to study the catalyst morphology. Z-contrast STEM micrographs (Fig. 4) help to

elucidate the structure and the metal distribution. Three images of Pd/C-CeO$_2$ are shown at various magnifications. Firstly, it is clear that the CeO$_2$ particles do not cover uniformly the Vulcan XC-72 carbon with distinct agglomerated CeO$_2$ structures that are separated from the Vulcan carbon (the CeO$_2$ agglomerates appear brighter on the STEM micrographs with respect to the carbon). It is difficult to individualize isolated Pd nanoparticles deposited on the ceria part of the support due to poor resolution between ceria and Pd nanoparticles. As a consequence the average Pd particle size distribution was determined by HR-TEM analysis only for the visible carbon supported particles (mean is 2.0 nm see SI).
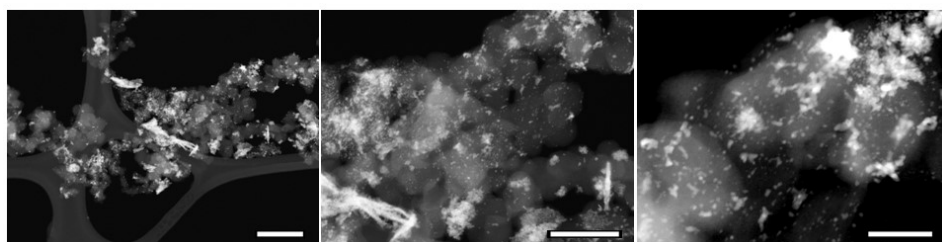


Fig. 4: STEM micrographs of the Pd/C-CeO$_2$ sample at different magnifications (scale bars from left to right; 200 nm, 100 nm and 50 nm respectively).

We used STEM-EDX (Energy Dispersive X-ray) elemental map analysis of representative portions of the catalyst to investigate the Pd distribution over both the carbon and ceria portions of the catalyst. In Figure 5 a typical portion of the catalyst is shown. A clear accumulation of Pd on the ceria regions is observed. This affinity can be justified by the fact that the conditions of high pH during synthesis gives rise to strong ionic interactions between the charged ceria surface and the Pd precursor cations in solution.[60, 61] Combined with the lipophilicity of the carbon part of the support these factors ultimately lead to the deposition of Pd nanoparticles on or near the ceria regions.
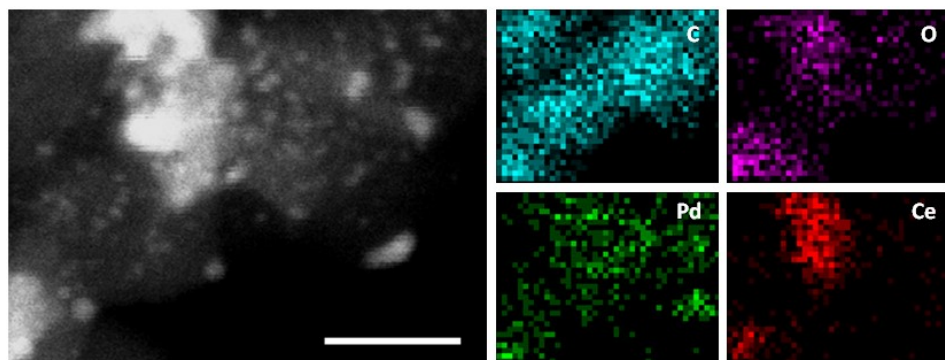
Fig. 5: STEM micrograph of the Pd/C-CeO$_2$ catalyst and related EDX maps for C, O, Pd and Ce respectively (scale bar is 20nm).

To look closer at the Pd-ceria interactions we used TEM and HRTEM (Figs 6a and c). The TEM images confirm small Pd particles of around 2nm diameter. In more detail (Fig. 6b), Pd particles are typically found in close proximity with both ceria particles and the Vulcan XC-72 support.
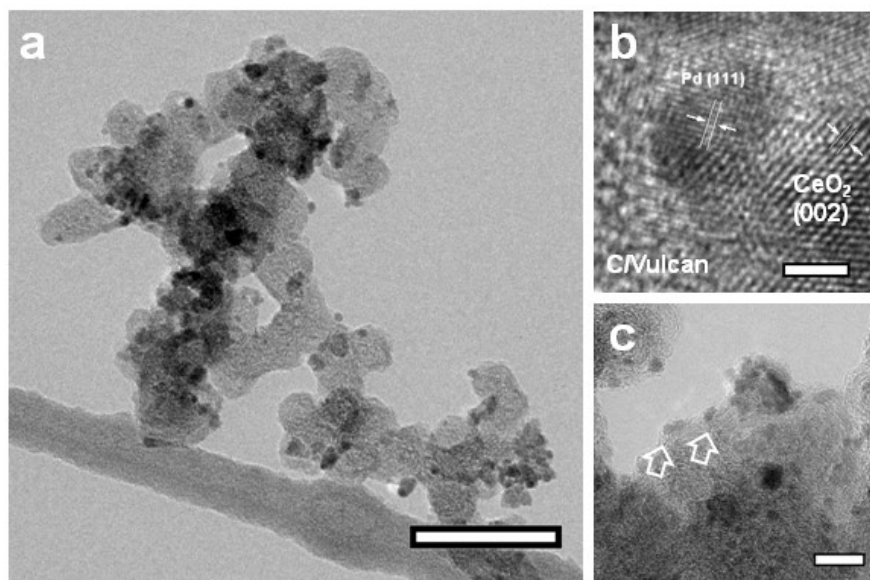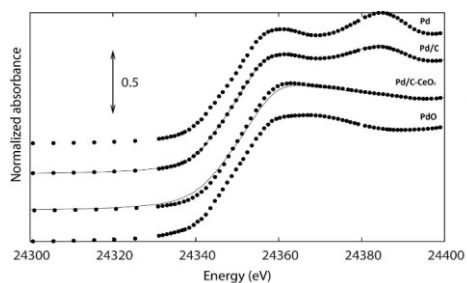
Fig. 6: (a) TEM image of Pd nanoparticle distribution on Pd/C-CeO$_2$ (scale bar is 50 nm) (b) a single Pd nanoparticle in contact with CeO$_2$ and Vulcan XC-72 carbon (scale bar is 2 nm); and (c) Pd NPs on a bare Vulcan XC-72 region of the sample (scale bar is 5 nm) indicated by arrows.

The Pd oxidation state in the Pd/C and Pd/C-CeO$_2$ catalysts was investigated by X-ray Absorption Spectroscopy (XAS). Spectra were also collected on PdO and on a foil of metallic Pd as standard materials for the valence state as in our previous investigations.[62] In Fig 7a a comparison of the XANES (X-ray Absorption Near Edge Structure) spectra clearly shows that Pd in Pd/C-CeO$_2$ is mostly oxidized, while in Pd/C the palladium is prevalently in its metallic state. EXAFS (Extended X-ray Absorption Fine Structure) analysis was carried out modeling the data with two components, i.e. metallic Pd and PdO. The metal was introduced with the first coordination shell whereas for the oxide two shells (Pd-O and second Pd-Pd) were considered. The raw EXAFS data and related Fourier Transforms are shown in Figs. 7b and 7c respectively. The EXAFS analysis shows Pd(II) accounts for 87 wt% of the total palladium content in Pd/C-CeO$_2$ (Table 2) which is unusual as carbon supported Pd NPs of small dimensions (e.g. 2 nm), have usually at least 50 wt% in the metallic state.[63] As expected only 17 wt% of PdO was found in the Pd/C system. A Table with the ~~first~~ considered coordination shell distances of palladium and the relative Debye Waller Factors (DWF) is reported in the supplementary info section (Table). The XAS data therefore shows for the C-CeO$_2$ supported catalyst that the Pd exists primarily as oxide. And this also confirms that Pd is preferentially supported on the ceria regions of the catalyst. In Pd NPs supported on CeO$_2$ the Pd-CeO$_2$ interaction is known to lead to oxidation of Pd through electron transfer to CeO$_2$.[60]
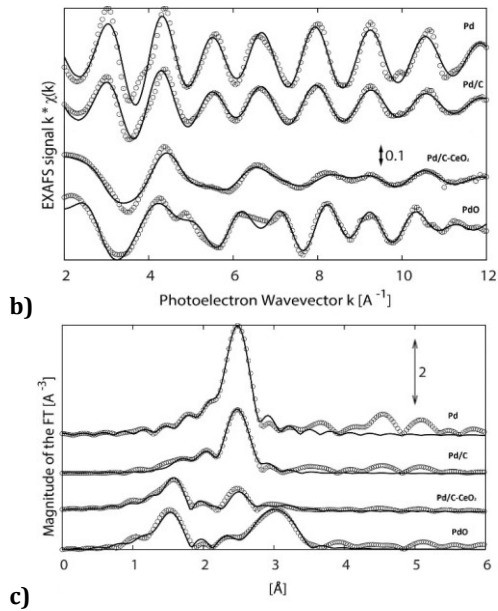


a)

**b)**



**c)**

Fig. 7. (a) XANES at the ~~Pd~~ Pd-Kα edge of Pd/C-CeO$_2$ , ~~and~~ Pd/C ~~(XANES spectra of~~ and model compounds Pd metal ~~foil~~ and PdO (dots). The spectra of the samples are reproduced as linar combinations of the model compounds (thin line), ~~are also shown)~~, (b) EXAFS data and the related (c) Fourier transforms at the Pd Kα edge (transformation range 2.8-13.5 Å$^{-1}$, k$^2$ weight). Dots represent the experimental data while the continuous lines represent the ~~calculated~~ best fi~~t~~st ~~data~~.

Table 2: Pd ~~oxidation state~~ speciation ~~distribution~~ (%) from ~~XAFS~~ EXAFS and XANES analysis. Relative uncertainties are listed in brackets.

|  | Pd metal | Pd oxide |
|---|---|---|
| Pd/C | 82(6) | 18(6) |
| Pd/C-CeO$_2$ | 13(5) | 87(5) |

In-situ XRPD was used to simulate the conditions at the anode electrode in the AEM-FC) under flowing H$_2$ gas at room temperature. The XRPD trace of the as-prepared catalyst at room temperature (Figure ~~9a~~8a) shows the signal associated with Pd metal at 2θ = 40° appears as a low intensity broad peak typical of a sample in which most of the Pd exists as ~~an amorphous oxide~~nanoparticles. On contact with a flowing 5% H$_2$ in Helium gas mixture the XRPD signal for Pd grows in intensity as the oxides are reduced to metallic Pd (9b).

Upon further contact with $H_2$ gas this peak shifts to a position representative of $H_2$ loaded Pd (9c).[64] After removing $H_2$ from the gas the signal for Pd shifts to the position of Pd metal (9d). This experiment demonstrates that Pd/C-CeO$_2$ (containing mostly PdO) is a precursor to the working catalyst, which forms upon reduction of the oxidized Pd surface upon contact with $H_2$ at the anode of the fuel cell.
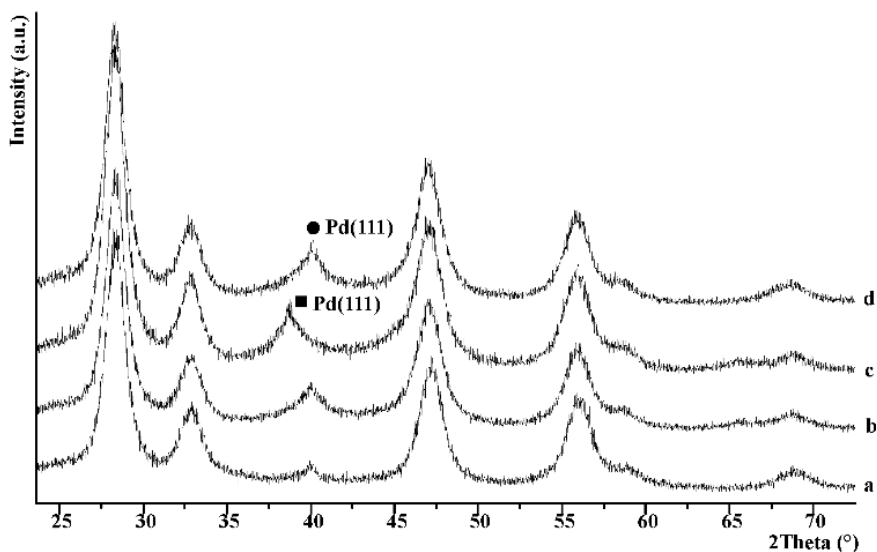


Fig. 98. In-situ XRPD traces of Pd/C-CeO$_2$ (a) synthesized catalyst, (b) initially under a flow of $H_2$ (5 %) in He, (c) afer a period of contact with H2 and (d) after switch to 100 % Helium

(● Pd (111) and ▇ $H_2$ loaded Pd (111). The other peaks in the XRPD traces are due to CeO$_2$.

The enhancement of the catalyst activity towards the HOR therefore requires finely dispersed and small Pd and CeO$_2$ nanoparticles in contact with each other (Schematically shown in Fig. 79). Indeed, we have seen that Pd preferentially accumulates on the ceria regions. The adsorbed OH species that accumulate on the CeO$_2$ particles are in close proximity to the Pd NPs thus allowing fast transfer to form Pd-OH$_{ad}$ sites which then react with the hydrogen intermediates (Pd-H$_{ad}$) that are adsorbed on the Pd surface.
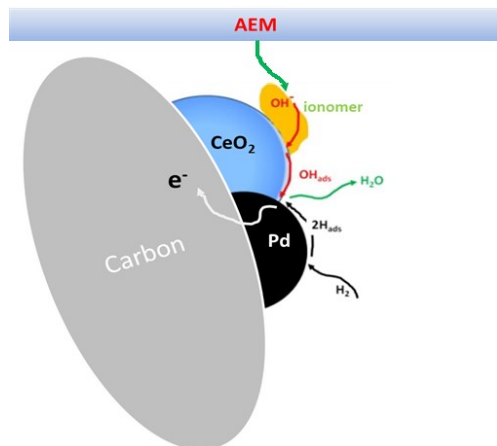
Fig. 8: Schematic diagram of the proposed ceria-Pd-carbon synergistic mechanism for HOR in AEM-FCs.

In summary, a Pd/C-CeO$_2$ anode catalyst has been developed and employed in a Pt-free AEM-FC. The presence of CeO$_2$ deposited onto the carbon support of a nanoparticle Pd catalyst leads to a 5 fold increase in performance as fuel cell anode with respect to a carbon only supported Pd catalyst. A careful analysis of the catalyst morphology shows a fine dispersion of the Pd nanoparticles accumulated mostly on the ceria portion of the catalyst. Such a structure leads to a weakening of the Pd-H binding energy and exploits the oxophilic nature of CeO$_2$ in supplying OH$_{ad}$ to the Pd-H$_{ad}$ HOR reaction sites, thus accelerating the overall HOR. An AEM-FC using this Pd/C-CeO$_2$ anode catalyst and an Ag cathode catalyst has been tested with dry hydrogen and partially filtered ambient air (<10 ppm CO$_2$) supplied to the anode and cathode, respectively. Peak power density output as high as 0.5 W cm$^{-2}$ with a maximum current density of 3 A cm$^{-2}$ is achieved with this Pt-free AEM-FC.

**References:**

1. M. K. Debe, *Nature*, 2012, **486**, 43-51.
2. M. K. Debe, 2011.
3. S. F. Lu, J. Pan, A. B. Huang, L. Zhuang and J. T. Lu, *P Natl Acad Sci USA*, 2008, **105**, 20611-20614.
4. M. Piana, M. Boccia, A. Filpi, E. Flammia, H. A. Miller, M. Orsini, F. Salusti, S. Santiccioli, F. Ciardelli and A. Pucci, *J Power Sources*, 2010, **195**, 5875-5881.
5. J. R. Varcoe and R. C. T. Slade, *Fuel Cells*, 2005, **5**, 187-200.
6. J. Suntivich, H. A. Gasteiger, N. Yabuuchi, H. Nakanishi, J. B. Goodenough and Y. Shao-Horn, *Nat Chem*, 2011, **3**, 546-550.
7. Y. J. Sa, C. Park, H. Y. Jeong, S. H. Park, Z. Lee, K. T. Kim, G. G. Park and S. H. Joo, *Angew Chem Int Edit*, 2014, **53**, 4102-4106.
8. D. Dekel, in *Encyclopedia of Applied Electrochemistry*, eds. G. Kreysa, K.-i. Ota and R. Savinell, Springer New York, 2014, ch. 524, pp. 33-45.
9. D. Dekel, in *Encyclopedia of Applied Electrochemistry*, eds. G. Kreysa, K.-i. Ota and R. Savinell, Springer New York, 2014, ch. 181, pp. 26-33.
10. J. R. Varcoe, P. Atanassov, D. R. Dekel, A. M. Herring, M. A. Hickner, P. A. Kohl, A. R. Kucernak, W. E. Mustain, K. Nijmeijer, K. Scott, T. W. Xu and L. Zhuang, *Energ Environ Sci*, 2014, **7**, 3135-3191.
11. L. Jiang, A. Hsu, D. Chu and R. Chen, *Electrochim Acta*, 2010, **55**, 4506-4511.
12. D. A. Slanac, W. G. Hardin, K. P. Johnston and K. J. Stevenson, *J Am Chem Soc*, 2012, **134**, 9812-9819.
13. J. Lee, B. Jeong and J. D. Ocon, *Curr Appl Phys*, 2013, **13**, 309-321.
14. R. Othman, A. L. Dicks and Z. H. Zhu, *Int J Hydrogen Energ*, 2012, **37**, 357-372.
15. I. Kruusenberg, L. Matisen, Q. Shah, A. M. Kannan and K. Tammeveski, *Int J Hydrogen Energ*, 2012, **37**, 4406-4412.
16. A. Brouzgou, S. Q. Song and P. Tsiakaras, *Appl Catal B-Environ*, 2012, **127**, 371-388.
17. F. Jaouen, E. Proietti, M. Lefevre, R. Chenitz, J. P. Dodelet, G. Wu, H. T. Chung, C. M. Johnston and P. Zelenay, *Energ Environ Sci*, 2011, **4**, 114-130.
18. *USA Pat.,* 8,637,196, 2014.
19. *USA Pat. Appl.,* 20130295485, 2013.

20. *USA Pat.,* 8,257,872, 2012.
21. *USA Pat.,* 7,943,258, 2011.
22. *Japan Pat.,* 5,520,968, 2014.
23. N. I. Andersen, A. Serov and P. Atanassov, *Appl Catal B-Environ*, 2015, **163**, 623-627.
24. Q. P. Hu, G. W. Li, J. Pan, L. S. Tan, J. T. Lu and L. Zhuang, *Int J Hydrogen Energ*, 2013, **38**, 16264-16268.
25. J. S. Guo, J. Zhou, D. Chu and R. R. Chen, *J Phys Chem C*, 2013, **117**, 4006-4017.
26. L. Ding, Q. Xin, X. J. Zhou, J. L. Qiao, H. Li and H. J. Wang, *J Appl Electrochem*, 2013, **43**, 43-51.
27. G. Lalande, G. Faubert, R. Cote, D. Guay, J. P. Dodelet, L. T. Weng and P. Bertrand, *J Power Sources*, 1996, **61**, 227-237.
28. L. Ding, J. L. Qiao, X. F. Dai, J. Zhang, J. J. Zhang and B. L. Tian, *Int J Hydrogen Energ*, 2012, **37**, 14103-14113.
29. H. A. Miller, M. Bevilacqua, J. Filippi, A. Lavacchi, A. Marchionni, M. Marelli, S. Moneti, W. Oberhauser, E. Vesselli, M. Innocenti and F. Vizza, *J Mater Chem A*, 2013, **1**, 13337-13347.
30. V. Bambagioni, C. Bianchini, J. Filippi, A. Lavacchi, W. Oberhauser, A. Marchionni, S. Moneti, F. Vizza, R. Psaro, V. Dal Santo, A. Gallo, S. Recchia and L. Sordelli, *J Power Sources*, 2011, **196**, 2519-2529.
31. M. Lefevre, E. Proietti, F. Jaouen and J. P. Dodelet, *Science*, 2009, **324**, 71-74.
32. E. Proietti, F. Jaouen, M. Lefevre, N. Larouche, J. Tian, J. Herranz and J. P. Dodelet, *Nat Commun*, 2011, **2**.
33. P. Trogadas, T. F. Fuller and P. Strasser, *Carbon*, 2014, **75**, 5-42.
34. Z. Yang, H. G. Nie, X. Chen, X. H. Chen and S. M. Huang, *J Power Sources*, 2013, **236**, 238-249.
35. K. P. Gong, F. Du, Z. H. Xia, M. Durstock and L. M. Dai, *Science*, 2009, **323**, 760-764.
36. USA Pat., 8,304,368, 2012.
37. Z. C. Wang, L. Xin, X. S. Zhao, Y. Qiu, Z. Y. Zhang, O. A. Baturina and W. Z. Li, *Renew Energ*, 2014, **62**, 556-562.
38. S. Maheswari, P. Sridhar and S. Pitchumani, *Electrocatalysis*, 2012, **3**, 13-21.
39. N. Wagner, M. Schulze and E. Gulzow, *J Power Sources*, 2004, **127**, 264-272.
40. J. R. Varcoe, R. C. T. Slade, G. L. Wright and Y. L. Chen, *J Phys Chem B*, 2006, **110**, 21041-21049.
41. E. Gulzow, N. Wagner and M. Schulze, *Fuel Cells*, 2003, **3**, 67-72.
42. A. Serov and C. Kwak, *Appl Catal B-Environ*, 2009, **90**, 313-320.
43. J. Zhang, S. H. Tang, L. Y. Liao and W. F. Yu, *Chinese J Catal*, 2013, **34**, 1051-1065.
44. N. Danilovic, R. Subbaraman, D. Strmcnik, A. P. Paulikas, D. Myers, V. R. Stamenkovic and N. M. Markovic, *Electrocatalysis*, 2012, **3**, 221-229.
45. W. C. Sheng, H. A. Gasteiger and Y. Shao-Horn, *J Electrochem Soc*, 2010, **157**, B1529-B1536.

46. J. Durst, A. Siebel, C. Simon, F. Hasche, J. Herranz and H. A. Gasteiger, *Energ Environ Sci*, 2014, **7**, 2255-2260.

47. V. Bambagioni, C. Bianchini, Y. X. Chen, J. Filippi, P. Fornasiero, M. Innocenti, A. Lavacchi, A. Marchionni, W. Oberhauser and F. Vizza, *Chemsuschem*, 2012, **5**, 1266-1273.

48. *USA Pat. Appl.*, 20100216052, 2010.

49. Y. Wang, G. W. Wang, G. W. Li, B. Huang, J. Pan, Q. Liu, J. J. Han, L. Xiao, J. T. Lu and L. Zhuang, *Energ Environ Sci*, 2015, **8**, 177-181.

50. S. St John, R. W. Atkinson, R. R. Unocic, T. A. Zawodzinski and A. B. Papandrew, *J Phys Chem C*, 2015, **119**, 13481-13487.

51. W. C. Sheng, Z. B. Zhuang, M. R. Gao, J. Zheng, J. G. G. Chen and Y. S. Yan, *Nat Commun*, 2015, **6**.

52. M. Shao, *J Power Sources*, 2011, **196**, 2433-2444.

53. P. J. Rheinlander, J. Herranz, J. Durst and H. A. Gasteiger, *J Electrochem Soc*, 2014, **161**, F1448-F1457.

54. Z. L. A. Feng, F. El Gabaly, X. F. Ye, Z. X. Shen and W. C. Chueh, *Nat Commun*, 2014, **5**.

55. T. Mori, D. R. Ou, J. Zou and J. Drennan, *Prog Nat Sci-Mater*, 2012, **22**, 561-571.

56. D. R. Ou, T. Mori, H. Togasaki, M. Takahashi, F. Ye and J. Drennan, *Langmuir*, 2011, **27**, 3859-3866.

57. H. F. Xu and X. L. Hou, *Int J Hydrogen Energ*, 2007, **32**, 4397-4401.

58. T. Skala, F. Sutara, M. Skoda, K. C. Prince and V. Matolin, *J Phys-Condens Mat*, 2009, **21**.

59. D. Strmcnik, M. Uchimura, C. Wang, R. Subbaraman, N. Danilovic, D. van der Vliet, A. P. Paulikas, V. R. Stamenkovic and N. M. Markovic, *Nat Chem*, 2013, **5**, 300-306.

60. W. J. Shen and Y. Matsumura, *J Mol Catal a-Chem*, 2000, **153**, 165-168.

61. M. L. Toebes, J. A. van Dillen and Y. P. de Jong, *J Mol Catal a-Chem*, 2001, **173**, 75-98.

62. L. Wang, A. Lavacchi, M. Bellini, F. D'Acapito, F. D. Benedetto, M. Innocenti, H. A. Miller, G. Montegrossi, C. Zafferoni and F. Vizza, *Electrochim Acta*, 2015, **177**, 100-106.

63. M. Suleiman, N. M. Jisrawi, O. Dankert, M. T. Reetz, C. Bahtz, R. Kirchheim and A. Pundt, *J Alloy Compd*, 2003, **356**, 644-648.

1. M. K. Debe, *Nature*, 2012, **486**, 43-51.

2. M. K. Debe, 2011.

3. S. F. Lu, J. Pan, A. B. Huang, L. Zhuang and J. T. Lu, *P Natl Acad Sci USA*, 2008, **105**, 20611-20614.

4. M. Piana, M. Boccia, A. Filpi, E. Flammia, H. A. Miller, M. Orsini, F. Salusti, S. Santiccioli, F. Ciardelli and A. Pucci, *J Power Sources*, 2010, **195**, 5875-5881.

5.      J. R. Varcoe and R. C. T. Slade, *Fuel Cells*, 2005, **5**, 187-200.

6.      J. Suntivich, H. A. Gasteiger, N. Yabuuchi, H. Nakanishi, J. B. Goodenough and Y. Shao-Horn, *Nat Chem*, 2011, **3**, 546-550.

7.      Y. J. Sa, C. Park, H. Y. Jeong, S. H. Park, Z. Lee, K. T. Kim, G. G. Park and S. H. Joo, *Angew Chem Int Edit*, 2014, **53**, 4102-4106.

8.      D. Dekel, in *Encyclopedia of Applied Electrochemistry*, eds. G. Kreysa, K.-i. Ota and R. Savinell, Springer New York, 2014, ch. 524, pp. 33-45.

9.      D. Dekel, in *Encyclopedia of Applied Electrochemistry*, eds. G. Kreysa, K.-i. Ota and R. Savinell, Springer New York, 2014, ch. 181, pp. 26-33.

10.     J. R. Varcoe, P. Atanassov, D. R. Dekel, A. M. Herring, M. A. Hickner, P. A. Kohl, A. R. Kucernak, W. E. Mustain, K. Nijmeijer, K. Scott, T. W. Xu and L. Zhuang, *Energ Environ Sci*, 2014, **7**, 3135-3191.

11.     L. Jiang, A. Hsu, D. Chu and R. Chen, *Electrochim Acta*, 2010, **55**, 4506-4511.

12.     D. A. Slanac, W. G. Hardin, K. P. Johnston and K. J. Stevenson, *J Am Chem Soc*, 2012, **134**, 9812-9819.

13.     J. Lee, B. Jeong and J. D. Ocon, *Curr Appl Phys*, 2013, **13**, 309-321.

14.     R. Othman, A. L. Dicks and Z. H. Zhu, *Int J Hydrogen Energ*, 2012, **37**, 357-372.

15.     I. Kruusenberg, L. Matisen, Q. Shah, A. M. Kannan and K. Tammeveski, *Int J Hydrogen Energ*, 2012, **37**, 4406-4412.

16.     A. Brouzgou, S. Q. Song and P. Tsiakaras, *Appl Catal B-Environ*, 2012, **127**, 371-388.

17.     F. Jaouen, E. Proietti, M. Lefevre, R. Chenitz, J. P. Dodelet, G. Wu, H. T. Chung, C. M. Johnston and P. Zelenay, *Energ Environ Sci*, 2011, **4**, 114-130.

18.     *USA Pat.*, 8,637,196, 2014.

19.     2013.

20.     2012.

21.     2011.

22.     *Japan Pat.*, 2014.

23.     N. I. Andersen, A. Serov and P. Atanassov, *Appl Catal B-Environ*, 2015, **163**, 623-627.

24.     Q. P. Hu, G. W. Li, J. Pan, L. S. Tan, J. T. Lu and L. Zhuang, *Int J Hydrogen Energ*, 2013, **38**, 16264-16268.

25.     J. S. Guo, J. Zhou, D. Chu and R. R. Chen, *J Phys Chem C*, 2013, **117**, 4006-4017.

26.     L. Ding, Q. Xin, X. J. Zhou, J. L. Qiao, H. Li and H. J. Wang, *J Appl Electrochem*, 2013, **43**, 43-51.

27.     G. Lalande, G. Faubert, R. Cote, D. Guay, J. P. Dodelet, L. T. Weng and P. Bertrand, *J Power Sources*, 1996, **61**, 227-237.

28.     L. Ding, J. L. Qiao, X. F. Dai, J. Zhang, J. J. Zhang and B. L. Tian, *Int J Hydrogen Energ*, 2012, **37**, 14103-14113.

29.     H. A. Miller, M. Bevilacqua, J. Filippi, A. Lavacchi, A. Marchionni, M. Marelli, S. Moneti, W. Oberhauser, E. Vesselli, M. Innocenti and F. Vizza, *J Mater Chem A*, 2013, **1**, 13337-13347.

30.     V. Bambagioni, C. Bianchini, J. Filippi, A. Lavacchi, W. Oberhauser, A. Marchionni, S. Moneti, F. Vizza, R. Psaro, V. Dal Santo, A. Gallo, S. Recchia and L. Sordelli, *J Power Sources*, 2011, **196**, 2519-2529.

31.     M. Lefevre, E. Proietti, F. Jaouen and J. P. Dodelet, *Science*, 2009, **324**, 71-74.

32.     E. Proietti, F. Jaouen, M. Lefevre, N. Larouche, J. Tian, J. Herranz and J. P. Dodelet, *Nat Commun*, 2011, **2**.

33.     P. Trogadas, T. F. Fuller and P. Strasser, *Carbon*, 2014, **75**, 5-42.

34.     Z. Yang, H. G. Nie, X. Chen, X. H. Chen and S. M. Huang, *J Power Sources*, 2013, **236**, 238-249.

35.     K. P. Gong, F. Du, Z. H. Xia, M. Durstock and L. M. Dai, *Science*, 2009, **323**, 760-764.

36.     2012.

37.     Z. C. Wang, L. Xin, X. S. Zhao, Y. Qiu, Z. Y. Zhang, O. A. Baturina and W. Z. Li, *Renew Energ*, 2014, **62**, 556-562.

38.     S. Maheswari, P. Sridhar and S. Pitchumani, *Electrocatalysis*, 2012, **3**, 13-21.

39.     N. Wagner, M. Schulze and E. Gulzow, *J Power Sources*, 2004, **127**, 264-272.

40.     J. R. Varcoe, R. C. T. Slade, G. L. Wright and Y. L. Chen, *J Phys Chem B*, 2006, **110**, 21041-21049.

41.     E. Gulzow, N. Wagner and M. Schulze, *Fuel Cells*, 2003, **3**, 67-72.

42.     A. Serov and C. Kwak, *Appl Catal B-Environ*, 2009, **90**, 313-320.

43.     J. Zhang, S. H. Tang, L. Y. Liao and W. F. Yu, *Chinese J Catal*, 2013, **34**, 1051-1065.

44.     N. Danilovic, R. Subbaraman, D. Strmcnik, A. P. Paulikas, D. Myers, V. R. Stamenkovic and N. M. Markovic, *Electrocatalysis*, 2012, **3**, 221-229.

45.     W. C. Sheng, H. A. Gasteiger and Y. Shao-Horn, *J Electrochem Soc*, 2010, **157**, B1529-B1536.

46.     J. Durst, A. Siebel, C. Simon, F. Hasche, J. Herranz and H. A. Gasteiger, *Energ Environ Sci*, 2014, **7**, 2255-2260.

47.     V. Bambagioni, C. Bianchini, Y. X. Chen, J. Filippi, P. Fornasiero, M. Innocenti, A. Lavacchi, A. Marchionni, W. Oberhauser and F. Vizza, *Chemsuschem*, 2012, **5**, 1266-1273.

48.     2010.

49.     Y. Wang, G. W. Wang, G. W. Li, B. Huang, J. Pan, Q. Liu, J. J. Han, L. Xiao, J. T. Lu and L. Zhuang, *Energ Environ Sci*, 2015, **8**, 177-181.

50.     S. St John, R. W. Atkinson, R. R. Unocic, T. A. Zawodzinski and A. B. Papandrew, *J Phys Chem C*, 2015, **119**, 13481-13487.

51.     W. C. Sheng, Z. B. Zhuang, M. R. Gao, J. Zheng, J. G. G. Chen and Y. S. Yan, *Nat Commun*, 2015, **6**.

52.     M. Shao, *J Power Sources*, 2011, **196**, 2433-2444.

53.     P. J. Rheinlander, J. Herranz, J. Durst and H. A. Gasteiger, *J Electrochem Soc*, 2014, **161**, F1448-F1457.

54.     Z. L. A. Feng, F. El Gabaly, X. F. Ye, Z. X. Shen and W. C. Chueh, *Nat Commun*, 2014, **5**.

55.     T. Mori, D. R. Ou, J. Zou and J. Drennan, *Prog Nat Sci-Mater*, 2012, **22**, 561-571.

56.     D. R. Ou, T. Mori, H. Togasaki, M. Takahashi, F. Ye and J. Drennan, *Langmuir*, 2011, **27**, 3859-3866.

57.     H. F. Xu and X. L. Hou, *Int J Hydrogen Energ*, 2007, **32**, 4397-4401.

58.     T. Skala, F. Sutara, M. Skoda, K. C. Prince and V. Matolin, *J Phys-Condens Mat*, 2009, **21**.

59.     D. Strmcnik, M. Uchimura, C. Wang, R. Subbaraman, N. Danilovic, D. van der Vliet, A. P. Paulikas, V. R. Stamenkovic and N. M. Markovic, *Nat Chem*, 2013, **5**, 300-306.

60.     W. J. Shen and Y. Matsumura, *J Mol Catal a-Chem*, 2000, **153**, 165-168.

61.     M. L. Toebes, J. A. van Dillen and Y. P. de Jong, *J Mol Catal a-Chem*, 2001, **173**, 75-98.

62.     L. Wang, A. Lavacchi, M. Bellini, F. D'Acapito, F. D. Benedetto, M. Innocenti, H. A. Miller, G. Montegrossi, C. Zafferoni and F. Vizza, *Electrochim Acta*, 2015, **177**, 100-106.

63.     W. J. Zhou, M. Li, O. L. Ding, S. H. Chan, L. Zhang and Y. H. Xue, *Int J Hydrogen Energ*, 2014, **39**, 6433-6442.

64.     M. Suleiman, N. M. Jisrawi, O. Dankert, M. T. Reetz, C. Bahtz, R. Kirchheim and A. Pundt, *J Alloy Compd*, 2003, **356**, 644-648.